33rd Annual International Conference of the IEEE EMBS
Boston, Massachusetts USA, August 30 - September 3, 2011

Segmentation of brain blood vessels using projections in 3-D CT angiography images

Danilo Babin, Ewout Vansteenkiste, Aleksandra Pižurica and Wilfried Philips

Abstract— **Segmenting cerebral blood vessels is of great importance in diagnostic and clinical applications, especially in quantitative diagnostics and surgery on aneurysms and arteriovenous malformations (AVM). Segmentation of CT angiography images requires algorithms robust to high intensity noise, while being able to segment low-contrast vessels. Because of this, most of the existing methods require user intervention. In this work we propose an automatic algorithm for efficient segmentation of 3-D CT angiography images of cerebral blood vessels. Our method is robust to high intensity noise and is able to accurately segment blood vessels with high range of luminance values, as well as low-contrast vessels.**

I. Introduction

The structure and position of blood vessels is of great importance for surgical and diagnostic purposes, and therefore presents a well researched field. Special attention is given to the determination of the position and access points of cerebral aneurysms and arteriovenous malformations (AVM). It is of utmost importance for surgery to precisely determine the exact positions of vessels going in and out of the malformation, as well as their radii, bending angles and entering directions. For this purpose it is essential to have a good segmentation algorithm capable of segmenting the blood vessels approaching the sub-pixel dimensions. It is also important to implement a fast segmentation algorithm in order for it to applicable during surgery when needed.

The current reviews on vessels extraction techniques [3], [4], [5] show that most techniques used in clinical purposes today are semi-automatic, often extensively relying on user interaction. A significant number of studies exist concerning the visualization of brain blood vessels and cerebral aneurysms and malformations [7], where most of them incorporate problem specific geometric models [6] which might have a problem with high vessel intensity range, as well as segmenting the inner structure of the aneurysms because of its highly unpredictable shape. Shape and flow driven methods [8] can also have these problems. Mathematical morphology techniques [1], [2] are also widely used for the segmentation of medical images, but they also usually require user intervention and are not able to cope with the wide range of blood vessel pixel intensities.

All authors are with Department of Telecommunications and Information Processing-TELIN-IPI-IBBT, Faculty of Sciences, Ghent University, Sint-Pietersnieuwstraat 41, B-9000 Ghent, Belgium.

A. Pižurica is postdoctoral research fellow of the Fund for Scientific research in Flanders (FWO)

Danilo Babin: dbabin@telin.ugent.be
Ewout Vansteenkiste: ervsteen@telin.ugent.be
Aleksandra Pižurica: sanja@telin.ugent.be
Wilfried Philips: philips@telin.ugent.be

In this paper we propose a segmentation algorithm which is an extension of our previous work [9]. The idea in our work is to measure the extent to which parameters of interest in the neighborhood with certain shape and size of a central pixel relate to the current (central) pixel. The use of circle and square shaped neighborhoods proved to be good for segmenting low resolution images, but can be computationally intensive. We solve this problem by using projections as neighborhoods of the current pixel, which are calculated much faster due to their linear shape. This method is applicable for segmenting both large data sets of blood vessels and also gives satisfactory results in representing the structure of malformations.

II. The proposed method

We design our method for the purpose of segmenting CT angiography images of brain blood vessels, although the method is applicable to other segmentation problems. The advantage of this imaging modality is that only the blood vessel structures are visible, which means that the segmented image will have only two labels, one for the blood vessels and another for the background. The disadvantage is that the blood vessel structures have wide range of gray scale values (from 25 to 255 out of 256 gray scale values), which makes the use of simple threshold techniques inapplicable in the presence of high intensity noise, as found in the images. For this reason we base our method on the combination of pixel neighborhood structure and intensities of the object intended for segmentation, as described in [9], where the circular and square-shaped neighborhoods were used. The segmentation was based on examining the average values at different neighborhood size and their comparison to the current pixel value. Although this method yields good results in segmentation of objects with low resolution, it is not suited for segmenting large scale images because of its high computation times.

The novelty we propose here is defining neighborhoods as projections (lines passing through the currently processed pixel, but excluding the currently processed pixel) and examining the characteristic function based on the combination of following elementary functions: minimum (min), maximum (max), average (avr) and mid-range (mdr, defined as the average of the minimum and maximum value). We compare neighborhood characteristic function values to the value of the currently processed pixel, but instead of varying the neighborhood size, we vary the direction of the projection based on the predefined angle value. The new value of the pixel is equal to the number of projections for which the

978-1-4244-4122-8/11/$26.00 ©2011 IEEE

characteristic function has a value lower than the value of the current pixel. We segment the image by thresholding the obtained transformed image, preferably by setting the threshold value to the number of existing projections, which is the maximum possible value.

Let $p \in \mathbb{Z}^2$ denote the pixel of image I in the discrete Cartesian grid with a value $f(p)$ from a range of discrete gray scale values $f(p) \in [f_{min}, ..., f_{max}]$. For a given point p of the image I, with coordinates (x_p, y_p) we define the projection at the angle $\alpha \in (0, 180]$ as in (1).

$$P_\alpha(p) : \{q \in I,\ q \neq p \mid y_q = kx_q + (y_p - kx_p)\}, \quad (1)$$

where $k = \tan\alpha$ is a function of the projection angle. From the definition in (1) it is obvious that the projection at a given angle α is equal to the line at the same angle, but excluding the currently processed pixel. For this set we define the segmentation function s as a combination of basic functions on the set $P_\alpha(p)$, as in (2):

$$s(P_\alpha(p)) = \frac{1}{N}\sum_{i=1}^{N} b_i(P_\alpha(p)), \quad (2)$$

where b_i denotes a function from a set of basic functions: minimum, maximum, average and mid-range functions. These functions have been chosen for the reason of fast computations, because their values can be easily updated at each step while advancing pixel by pixel through the image. This is because they do not require additional memory space and its sorting, which would increase the computation time as in the case of median value calculation.

In (3) we define the projection set $S_n(p)$ containing n number of projections of point p with applied segmentation function s:

$$S_n(p) = \left\{ s(P_{i\frac{180}{n}}(p)), \quad i = \{1, ..., n\} \right\} \quad (3)$$

A projection set is illustrated in Fig. 1(b) for a single point of the original image in Fig. 1(a). We assign in (4) the new pixel value $d(p)$ as the number of projections contained in the projection set $S_n(p)$ of the pixel p for which the segmentation function value does not exceed the value of the pixel p:

$$d_n(p) = card(S'_n(p)), \quad (4)$$

where the $S'_n(p)$ represents the set of calculated segmentation function values which do not exceed the value of the processed pixel, as defined in (5):

$$S'_n(p) = \{s(P_\alpha(p)) \in S_n(p), \quad s(P_\alpha(p)) < f(p)\}. \quad (5)$$

A. Selecting the threshold value

In order to segment the image, we need to apply thresholding to the obtained transformed image. For the sake of keeping the method automatic, we set the threshold value to maximum value n, which means that only those pixels remain which are segmented for all projection directions. According to this, the threshold function is given in (6):

$$L_n(p) = \begin{cases} 1, & d_n(p) = n \\ 0, & d_n(p) < n \end{cases} \quad (6)$$

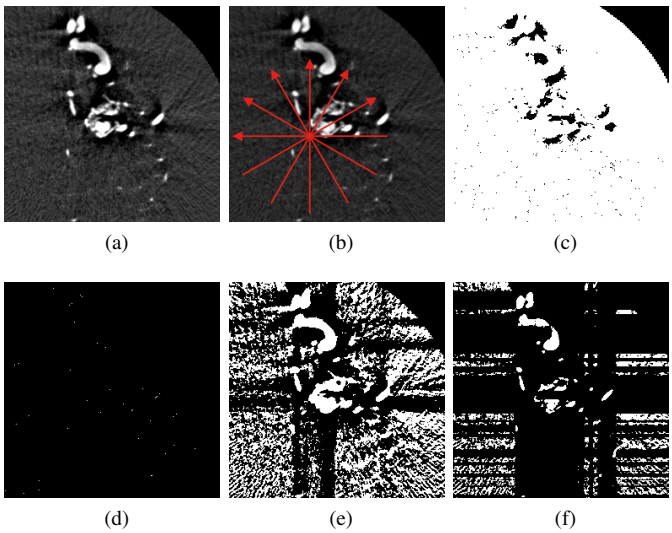

Fig. 1: Original image in (a), illustration of the projection set $S_n(p)$ in (b) and segmentation of the original image using two projections for the following basic functions: minimum (min) in (c), maximum (max) in (d), average (avr) in (e) and mid-range (mdr) in (f).

Because of using the largest possible threshold value, it is essential to correctly choose the segmentation function in order for all the objects in the image to get segmented.

B. Segmentation function selection

The segmentation function s has to be chosen so that it minimizes the number of projections needed for the segmentation of the image, but preserves all the important parts of the object for segmentation while eliminating noise in the image. A segmentation example using basic functions $s = b_i$ with two projections $n = 2$ is shown in Fig. 1. The results illustrated in Fig. 1 show that neither of the basic functions fulfills the requirements needed for the optimal segmentation. The minimum function shown in Fig. 1(c) segments a too large region, the maximum function in Fig. 1(d) segments too few pixels, the average function in Fig. 1(e) preserves details, but segments also too much noise and the mid-range function in Fig. 1(f) eliminates noise, but also removes some of the regions which should be segmented. For this reason, we examine a variety of segmentation functions obtained by combining the basic functions as defined in (2). Our examination shows that the best function for the purpose of segmenting our 3-D data sets is $s = (mdr{+}avr{+}max)/3$, because it proved to remove the most of the noise while preserving all the relevant objects in the image. The function can be easily chosen by testing the segmentation on a single slice of the hole 3-D data set.

C. Setting the number of projections

It is obvious that the transformation and segmentation results will depend on the number of projection directions. In the case of images with high pixel and inter-slice resolution and acceptable level of noise and artifacts, the number of

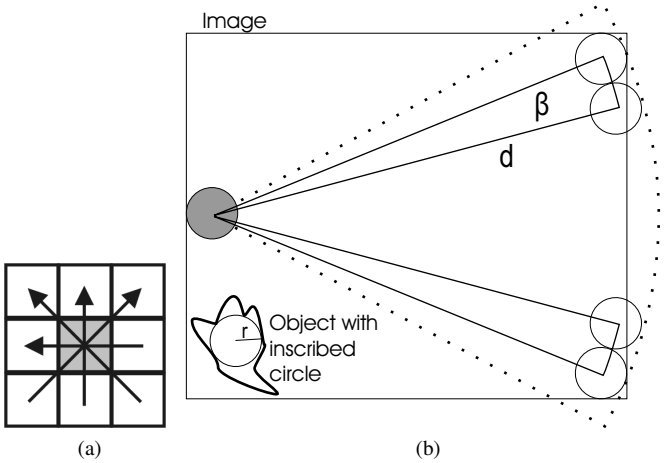

(a) (b)

Fig. 2: Four projections are enough for separation of the current pixel from its neighborhood as shown in (a), the number of projections to cover all image is defined by the inscribed circle of the largest object and the distance d of the corners to the center bottom position of the circle as shown in (b).

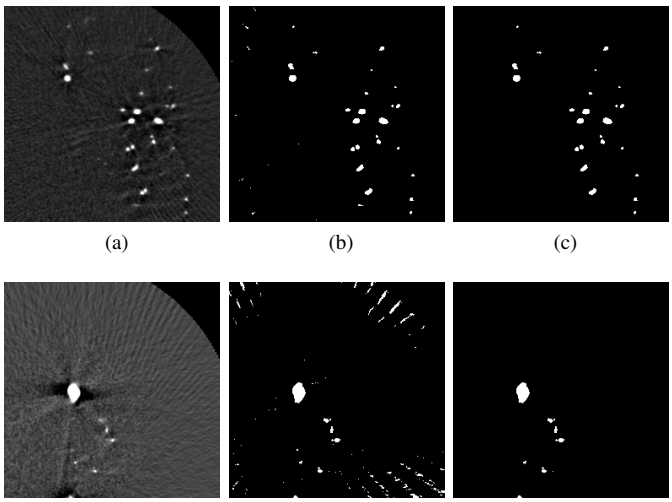

(a) (b) (c)

(d) (e) (f)

Fig. 3: Original images are in (a) and (d), corresponding transformed images with visible object and noise segments are in (b) and (e) and corresponding segmentation by extrapolation of the largest region is in (c) and (f).

projections can be set to its minimum value if the segmentation function is able to distinct between the object and the background without merging any segmented noise to the object. In this case, we need only four projections to get object distinction, since all the surrounding pixels in the eight neighborhood of the current pixel will be involved in these projections, as shown in Fig. 2(a). Although this method results in segmentation of large quantity of noise, all the surrounding pixels of the object are involved in projection calculation, which results in clear distinction between segmented object and noise.

In order for all the noise to be eliminated in the segmentation process, there must be a projection containing at least one object pixel for every pixel in the image. Because of this, the number of projections depends on the shape and size of the object for segmentation, as well as number of objects in the image. For simplicity reasons, we will approximately determine the number of projections corresponding to the largest inscribed circle of the largest object with the radius r for segmentation because it covers the same width of projection for each angle, which is not the case for other object shapes. We assume the position of the object which results in the largest number of directions, which happens when the object is centered at the shorter side of the image, as shown in Fig. 2(b). We take into account the largest distance d from this position, which is in the opposite corners of the image and according to it we determine the angle between the circle objects β, as in (7):

$$\beta = 2 \arcsin\left(\frac{r}{d}\right). \tag{7}$$

According to this, we determine the number of projections n as in (8):

$$n = \left\lceil \frac{\pi}{\beta} \right\rceil, \tag{8}$$

where the devision result is rounded to the first greater value. Since the segmentation function is well chosen, the number of projections can be a value somewhat larger than four and constant for all slices of the 3-D set. In this work we set the number of projections to $n = 16$, which is enough to include in the calculation neighboring pixels of an object within the radius of five pixels with all the listed problems. The results of transformation with listed parameters for the original images in Fig. 3(a) and Fig. 3(d) are shown in Fig. 3(b) and Fig. 3(e), respectively. The transformed image in Fig. 3(e) has a lot of segmented noise because of the small object area present in the original image, but the noise segments are situated further away from the object segments because of sufficient number of projections. On the other hand, the transformed image in Fig. 3(b) has a significantly larger object area and because of that noise segments are less present.

D. Algorithm for 3-D segmentation

A 3-D segmentation algorithm can be realized by extending a 2-D version of the proposed method to the 3-D space, but the method would be computationally demanding for large data sets, which would significantly prolong the execution time. Therefore, we use the proposed 2-D algorithm for the segmentation of the 3-D set with constant number of projections and fixed one segmentation function for the whole 3-D set. After the image transformation, a binary image is obtained containing both segmented object and segmented noise as presented in Fig. 3(b) and Fig. 3(e), but the two of these do not merge at any point. We extract

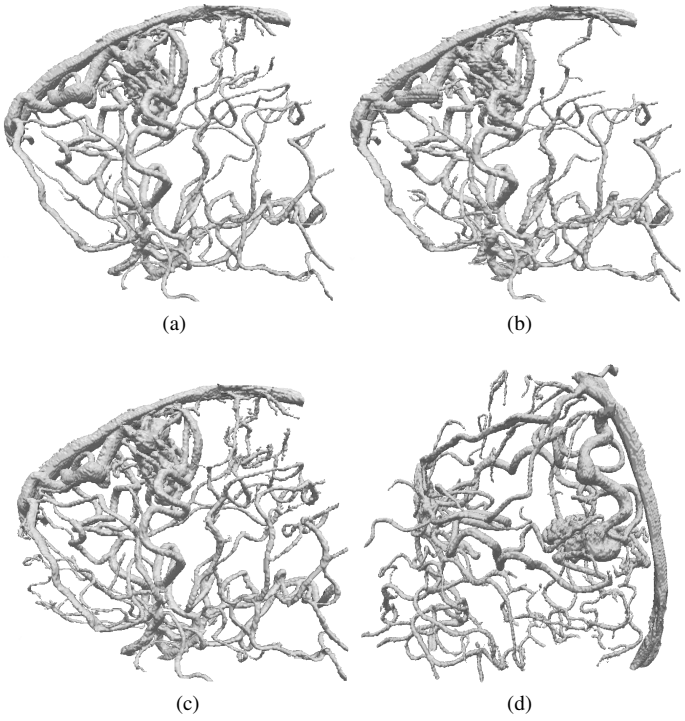

Fig. 4: Results of blood vessel segmentation obtained by: (a) connected components method, (b) morphological profiles and (c), (d) our proposed method. The results clearly show that our proposed method segments the most blood vessels of all the methods, with the aneurysm clearly visible in the middle of the blood vessel tree structure.

the object by finding the largest 3-D region in the image and discarding all the smaller regions, as shown in Fig. 3(c) and Fig. 3(f) for the transformed images in Fig. 3(b) and Fig. 3(e), respectively. From the obtained images we can see that no noise segments are present in the final segmentation.

III. Results

We tested our algorithm on six data sets of CT angiography images of brain blood vessels, using constant number of projections $n = 16$ and the segmentation function $s = (mdr + avr + max)/3$. We compare our method to connected components method [10], which is a method based on adaptive threshold setting and classical morphological profiles [11], where the segmentation is obtained by varying the size of given structuring element. For comparison reasons, we use the artificial phantom spiral model shown in Fig. 5a with added CT artifacts and noise. The connected components method (see Fig. 4a) segments more branches than the morphological profiles (see Fig. 4b), while our presented method segments the most of the blood vessel tree structure (see Fig. 4c) and phantom model (see Fig. 5).

The results presented in Fig. 4c and Fig. 4d show that the blood vessels were accurately segmented with clearly visible arterious and venous structures with the aneurysm in the center of the blood vessel tree.

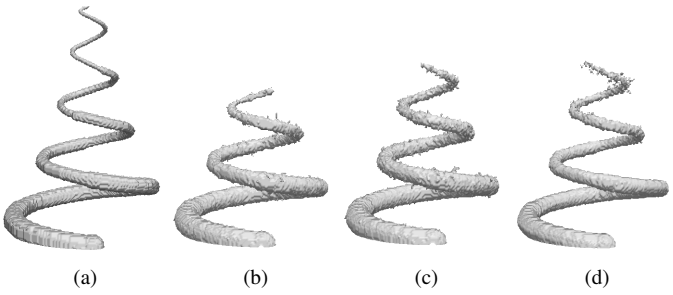

Fig. 5: Comparison of different techniques on the groundtruth 3-D image in (a). Both the MP method (b) and connected components (b) segment either smaller part of the spiral or introduce more noise to segmentation than our method in (d).

IV. Conclusion

We introduced a novel segmentation method based on projections for both 2-D and 3-D images with an application to segmentation of CT angiography images of brain blood vessels. We have explained the choice of the segmentation function and the determination of number of projections. Once these parameters are fixed, the algorithm works completely automatically. Our choice of basic segmentation functions used to generate the combined segmentation function significantly decreases computation time making it efficient for use on large 3-D data sets. Our method stands out in cases of segmentation of objects with high range luminance values, as well as in images with high noise values which often occurs in CT images. Obtained segmentation results show exact blood vessel tree structure and the best segmented phantom model of all the comparison methods.

References

[1] J. Serra: *Image Analysis and Mathematical Morphology*, volume 1, Academic Press, 1982.

[2] P. Soille: *Introduction to Mathematical Morphology*, Comput. Vis., Graph., Image Process., vol. 35, pages 283-305, 1986.

[3] C. Kirbas, F.K.H. Quek: *A Review of Vessel Extraction Techniques and Algorithms*, ACM Computing Surveys 36 (2), p. 81-121, 2004.

[4] Z. Yaniv, K. Cleary: *Image Guided Procedures: A Review*, Computer Aided Interventions and Medical Robotics, 2006.

[5] D. Lesage, E.D. Angelini, I. Bloch, G. Funka-Lea: *A review of 3D Vessel Lumen Segmentation Techniques: Models, Features and Extraction Schemes*, Medical Image Analysis, Elsevier, 2009.

[6] M. Piccinelli, A. Veneziani, D.A. Steinman, A. Remuzzi, L. Antiga: *A Framework for Geometric Analysis of Vascular Structures: application to Cerebral Aneurysms*, IEEE Transactions on Medical Imaging, 1141-1155, August 2009.

[7] L. Antiga, D.A. Steinman: *Vascular Modeling Toolkit*, Available on line: http://www.vmtk.org, January 2006.

[8] D. Nain, A. Yezzi, G. Turk: *Vessel Segmentation Using A Shape Driven Flow*, .

[9] D. Babin, E. Vansteenkiste, A. Pižurica, W. Philips: *Segmentation and length measurement of the abdominal blood vessels in 3-D MRI images*, EMBC 2009 Proceedings:

[10] J. De Bock, W. Philips: *Fast and Memory Efficient 2D Connected Components Using Linked Lists of Line Segments*, accepted for publication in IEEE Transactions on Image Processing.

[11] M. Pesaresi, J.A. Benediktsson: *A New Approach for the Morphological Segmentation of High-Resolution Satellite Imagery*, IEEE Trans. Geosci. Remote Sens., vol.39, no. 2, Feb. 2001.